BNL-104888-2014-TECH

AGS/AD/Tech Note No. 482;BNL-104888-2014-IR

Electron Impact Capture and Ionization Cross Sections

S. Y. Zhang

December 1998

Collider Accelerator Department

Brookhaven National Laboratory

U.S. Department of Energy

USDOE Office of Science (SC)

DISCLAIMER

For Internal Distribution Only

Accelerator Division
Alternating Gradient Synchrotron Department
BROOKHAVEN NATIONAL LABORATORY
Upton, New York 11973

Accelerator Division
Technical Note

AGS/AD/Tech. Note No. 482

Electron Impact Capture and Ionization Cross Sections

S.Y. Zhang

December 1998

I. Summary

1. Semi-empirical formulae for electron impact capture and ionization cross sections are given, based on the survey of theoretical and experimental results.
2. For Au^{31+} Booster injection, the capture loss is dominated.
3. For Au^{14+} Booster injection, the ionization loss would happen.

II. Introduction

For the electron impact capture cross section, the semi-empirical formula proposed in [1] is adopted. The comparison of this formulation is made with respect to the Bohr-Lindhard equation [2,3].

For the electron impact ionization cross section, the Lotz formula [4] is adopted.

Gold beam loss mechanism at the Booster injection is then discussed. It is found that for Au^{31+}, the capture loss is dominated. The situation is different for Au^{14+} Booster injection, where the ionization loss would happen.

In this article, the capture and ionization cross sections are given under the condition of electron impact. There are two reasons to use the cross section of electron impact. Firstly, the abundant electron impact experiments data can be directly used for verification. Secondly, it is straightforward to use these results to estimate the cross sections for different residual gas components, within a reasonable range of accuracy.

III. Electron impact capture cross section

In [1], a semi-empirical formula for electron impact capture cross section is proposed as,

$$\sigma_c = \frac{0.4q^{3.25}}{q^{2.25} + 2.56 \times 10^{-4} q^{1.25} E_k^2 + 9.05 \times 10^{-8} E_k^{4.5}} \log(\frac{2.44 \times 10^6 q^{0.5}}{E_k}) \quad (1)$$

where q is the projectile charge state, and E_k is the kinetic energy of projectile in unit of KeV/u. The unit of the capture cross section σ_c is $10^{-16}\ cm^2$. Let us call (1) as KMJ model.

The experiments in agreement with this formula include the follows,

1. Electron capture of Li^{3+} in a range of 100 eV/u to 200 KeV/u, and C^{6+} in a range of 100 eV/u to 200 KeV/u [5].
2. Ne^{10+} in a range of 20 KeV/u to 200 KeV/u, and Si^{14+} in a range of 20 KeV/u to 1 MeV/u [6].
3. H^{+}, He^{2+}, Li^{3+}, B^{5+}, C^{6+}, and Fe^{20+} in a range of 20 KeV/u to 4 MeV/u [7].
4. Ti^{3+} and Ti^{4+} in a range of 1 KeV/u to 100 KeV/u [8].
5. He^{2+}, Li^{3+}, B^{4+}, B^{5+}, C^{6+}, N^{7+}, $O^{8+}$and Fe^{20+} in a range of $<$ 100 KeV/u [9].
6. Ti^{22+}, $V^{23+}$and Fe^{26+} in a range of 400 KeV/u to 900 KeV/u [10].

In [1], capture cross sections of Ti ion from $q = 4$ to 11, Cr ion from $q = 4$ to 15, Fe ion from $q = 4$ to 26, and Ni ion from $q = 4$ to 17 have been calculated in agreement with (1).

Furthermore, it was found that in a scaling of the projectile energy by dividing $\sqrt{q}$, and the cross section by dividing q, unified cross sections can be obtained. This is shown in Fig.1a [1]. In Fig 1b, σ_c calculated by (1) is shown for comparison.

IV. Comparison with Bohr-Lindhard equation

In the Bohr-Lindhard equation [2,3], the capture cross section is described as,

$$\sigma_c = \pi a_0^2 Z_T^m q^2 \left(\frac{v}{v_0}\right)^{-\ell} \tag{2}$$

where $a_0 = 5.3 \times 10^{-9}$ cm is the Bohr radius, Z_T is the atomic number of residual gas. The Bohr velocity $v_0 = 2.19 \times 10^8$ cm/s ($\beta = 0.0073$) is the orbital velocity of the valence electrons of atoms in the target. The index ℓ is about 6, and $m \leq 1$.

This formulation gives clear dependance of the cross section on v and q. Unfortunately, large discrepancies in the dependance is not resolved. For

instance, the index ℓ referred can be in a range from 3 to 12. This makes the Bohr-Lindhard equation difficult to use.

In Fig.2, the comparison of (1) and (2) is given, where we take $\ell = 6$ for Bohr-Lindhard equation. Some discrepancies can be observed. At the Booster injection energy, which corresponds to $\beta = 0.044$, the difference is large.

At the low energy, the difference of KMJ model and Bohr-Lindhard model is large. This can be observed in Fig.2, for $\beta < 0.02$. We note that most experiments reported in [6-10] are in agreement with the KMJ model, rather than the Bohr-Lindhard model.

Also, using Bohr-Lindhard model, the small capture loss in electron cooling [11] cannot be explained, since the capture cross section would be extremely large in that case according to (2). Meanwhile, since the beam loss is also proportional to β, therefore, the flattened capture cross section at the low energy of KMJ model in fact implies that the loss in electron cooling would be small.

Therefore, we adopt the KMJ model for electron impact capture cross section calculation.

V. Electron impact ionization cross section

It is believed that the Lotz formulation [4] for electron impact ionization cross section is often within 20% of more accurate quantal calculations for direct ionization [12]. Therefore, we simply adopt this formulation,

$$\sigma_{ion} = 4.5 \times 10^{-14} \sum_{i=1}^{N} q_i \frac{\log(E_{ek}/P_i)}{E_{ek} P_i} \tag{3}$$

where E_{ek} is the kinetic energy of the incident electron in eV, P_i is the binding energy of electrons in the ith subshell in eV, q_i is the number of equivalent electrons in the ith subshell.

We note that the velocity of projectile with respect to the target is represented by E_{ek} of the incident electron in eV, since the ionization is identical in frame of moving impact electrons (ion as target) or in frame of moving ions (electron as target), where the latter is relevant to our case.

The binding energy of electrons of all states of ionization are available, for instance see [13], therefore, these data are directly used in calculating (3).

Various experiment data in agreement with this formulation can be found in [14].

The electron impact ionization cross sections for gold ions, relevant to gold beam Booster injection, are shown in Fig.3.

The comparison of capture and ionization cross sections of gold ions within the relevant range of Booster injection is shown in Fig.4.

VI. $Au^{31+}$and Au^{14+} Booster injection

Using the equation (1) and (3), the gold beam Booster injection with $Au^{31+}$and Au^{14+} is shown in Fig.5. The cross sections are larger if the particles are other than electrons. For instance, the nitrogen equivalent (N_2) residual gas capture and ionization cross sections are roughly as large as 14 times the electron impact cross sections.

We have the following comments,

1. For Au^{31+} Booster injection, the dominant beam loss mechanism is the capturing. Therefore, if the injection energy can be elevated, the beam injection efficiency can be improved. In specific, if the beam injected at $\beta = 0.0484$, and 0.055, i.e. increase 10% and 25% from $\beta = 0.044$, the electron capture cross section becomes $\sigma_c = 6.63 \times 10^{-18}$, and $2.06 \times 10^{-18}\ cm^2$, i.e., reduced by 58% and 87% from $\sigma_c = 1.573 \times 10^{-17}$, respectively.

2. For Au^{14+} Booster injection, both capture and ionization will happen. However, shortly after the energy ramped up, the ionization becomes dominant.

3. The beam life time is proportional to the product of cross section and the beam velocity, β. If the capture is dominant, then the beam life time improves as the beam energy ramping up, due to the fast reduction of capture cross section. If ionization is dominant, then the beam life time improvement is less significant, since the ionization cross section reduction is roughly in an order of β^{-1}, multiplying β, the loss becomes irrelevant with the beam energy.

4. The absolute cross sections shown in this article are somehow larger than it was believed early on, in connection to the Booster injection.

VII. Acknowledgment

The author would like to thank L.A. Ahrens, E. Beebe, and H.C. Hseuh for valuable discussions.

References

[1]K. Katsonis, G. Maynard and R.K. Janev, Physica Scripta, **T-37**, 80 (1991).

[2]H.D. Betz, Rev. Modern Phy. **44**, 465 (1972).

[3]H.C. Hseuh, Booster Tech. Note, No.116, Apr. (1988).

[4]W. Lotz, Z. Phys. **206**, 205 (1967).

[5]H. Ryufuku and T. Watanabe, Phys. Rev. **A-19**, 1538 (1979).

[6]H. Ryufuku and T. Watanabe, Phys. Rev. **A-20**, 1828 (1979).

[7]J. Eichler, Phys. Rev. **A-23**, 498 (1981).

[8]W. Fritsch, Physica Scripta, **T-37**, 75 (1991).

[9]N. Toshima, Phys. Rev. **A-50**, 3940 (1994).

[10]M. Das et. al. Phys. Rev. **A-52**, 4616 (1995).

[11]J. Bosser, CERN 95-06, 673 (1995).

[12]J.S. Thompson and D.C. Gregory, Phys. Rev. **A-50**, 1377 (1994).

[13]T.A. Carlson et. al. Atomic Data, **2**, 63 (1970).

[14]M.A. Lennon et. al. J. Phys. Chem. Ref. Data, **17**, No.3, 1285 (1988).

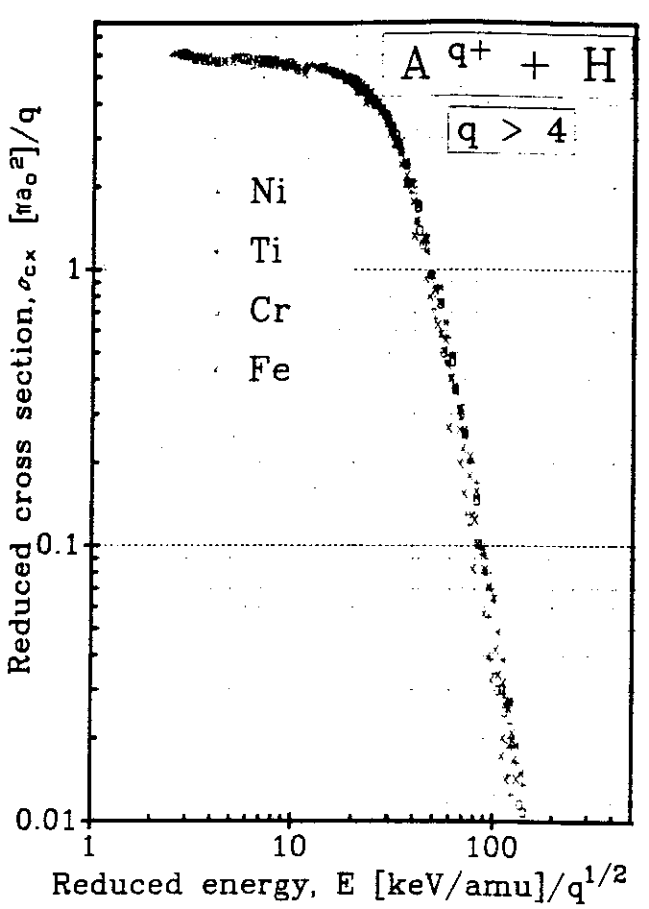

Fig. 5. Reduced charge exchange cross sections, σ_{cx}/q, vs. reduced collision energy, $E/q^{0.5}$, for the Ti^{q+}, Cr^{q+}, Fe^{q+} and Ni^{q+} ($q > 4$) collisions with H(1*s*).

a

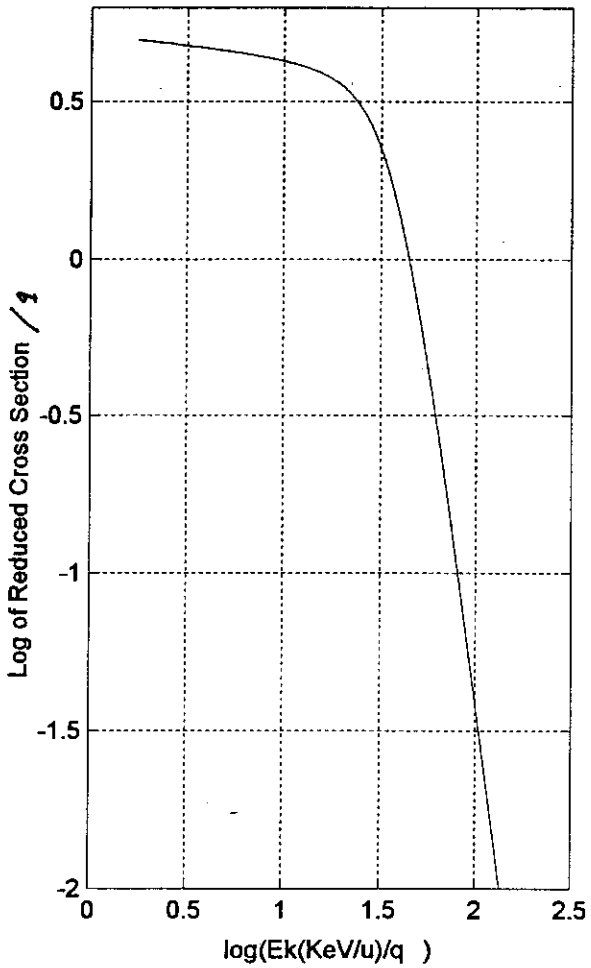

b

Fig.1. *Unified Capture Cross Section,*
projectile energy divided by $\sqrt{q}$, cross section divided by q

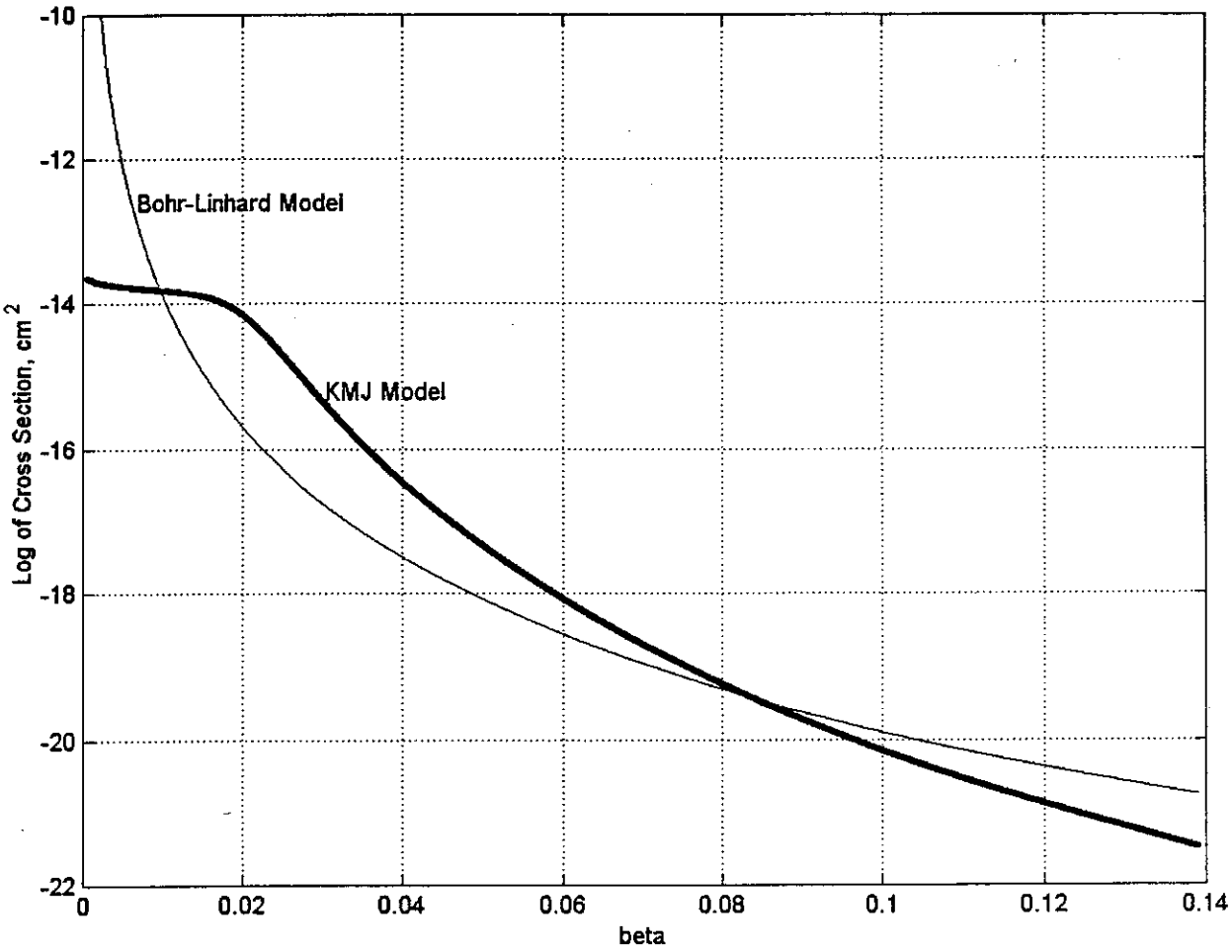

Fig.2. *Comparison of KMJ model and Bohr-Lindhard model*

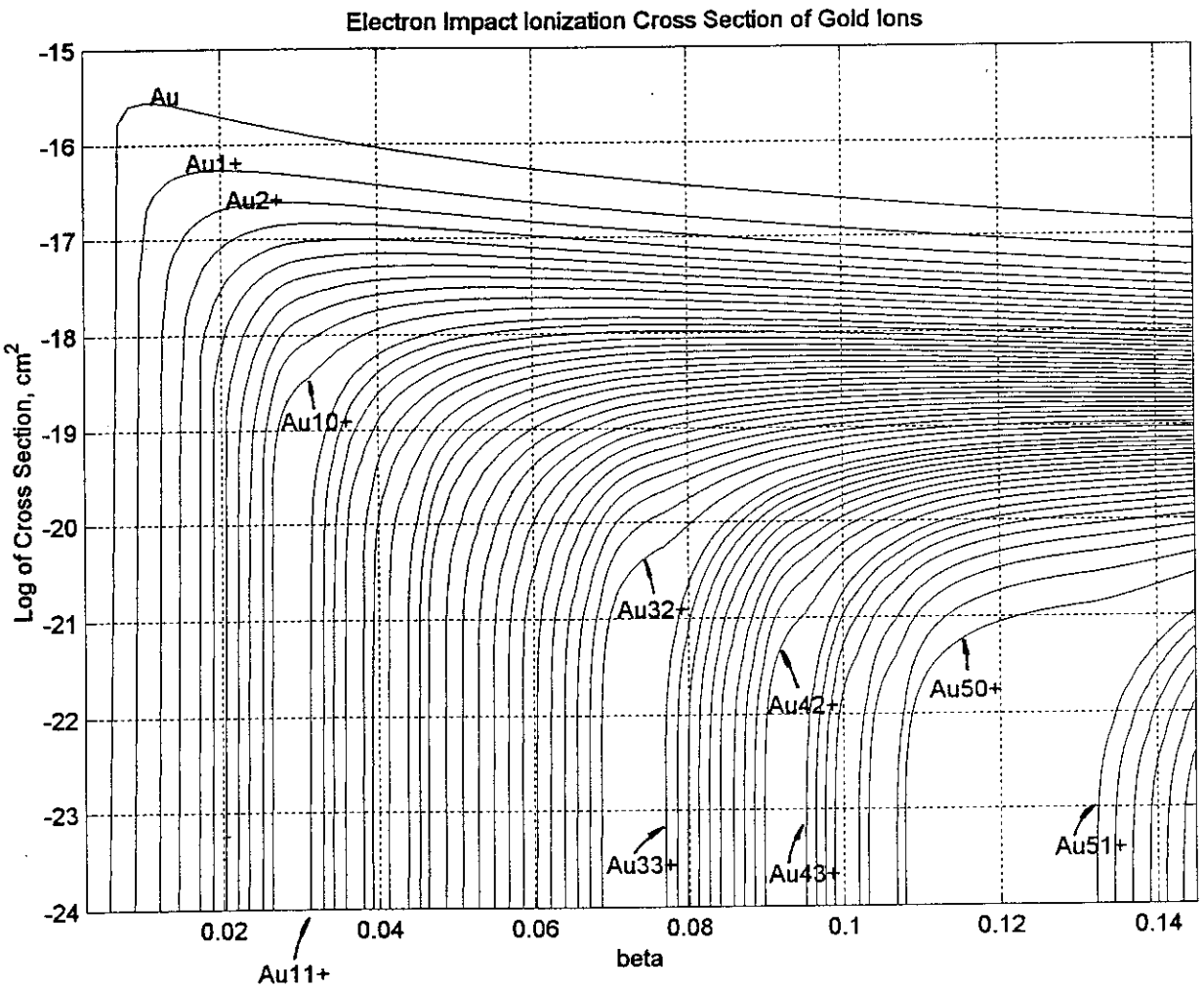

Fig.3. *Electron Impact Ionization Cross Section of Gold Ions*

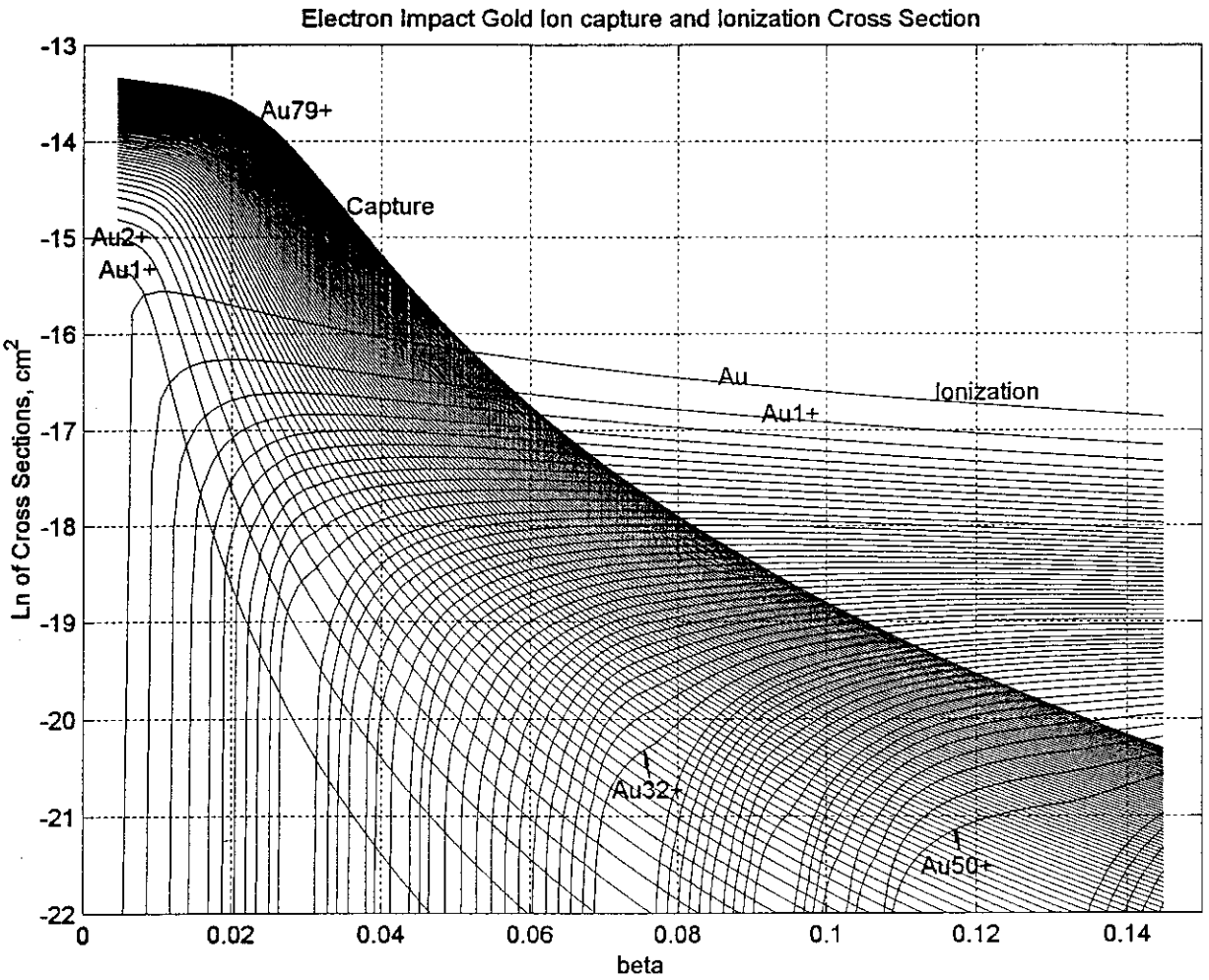

Fig.4. *Electron Impact Gold Ion Capture and Ionization Cross Sections*

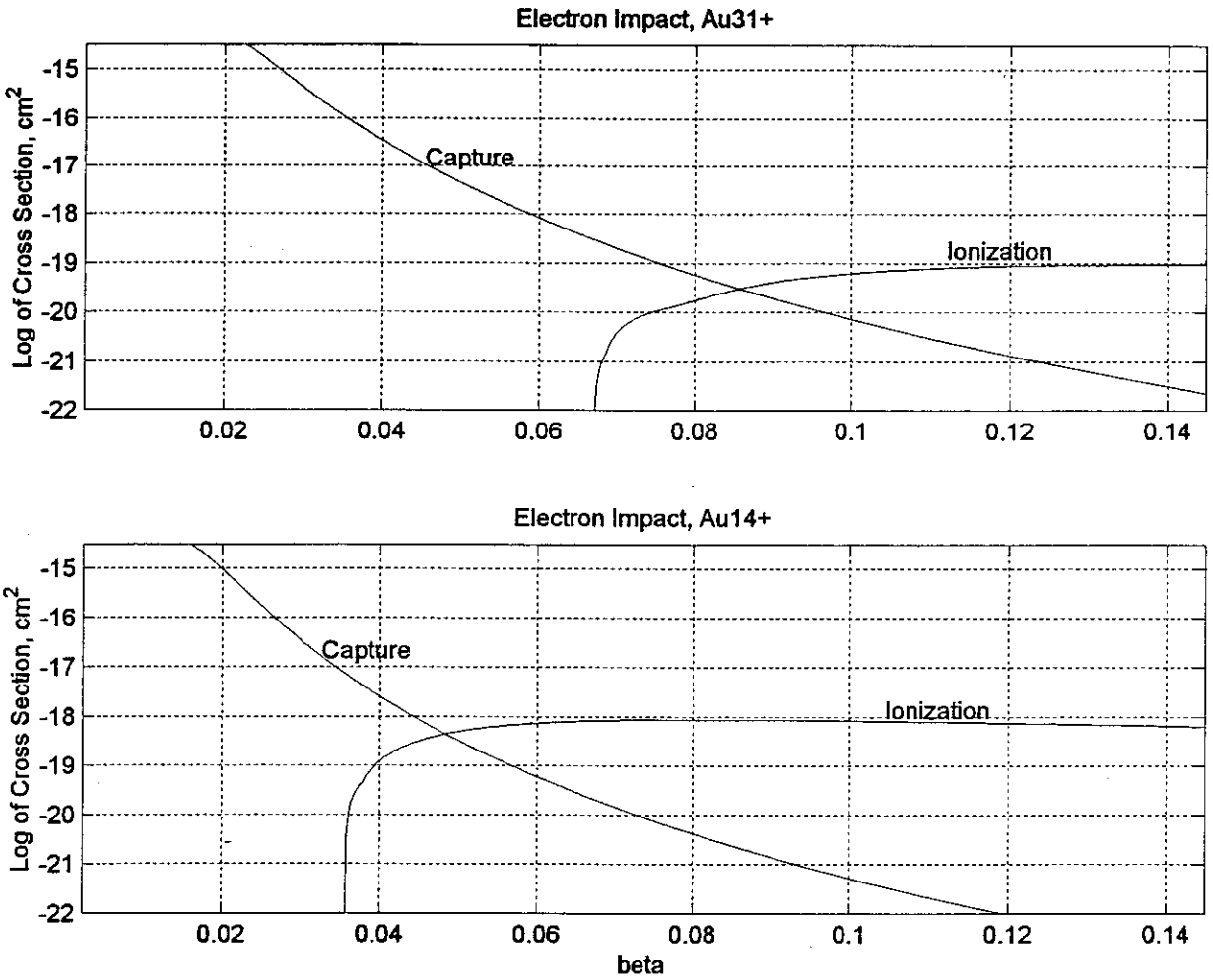

Fig.5. *Electron Impact Capture and Ionization Cross Sections for* Au^{31+} and Au^{14+}